Unsteady Transonic Flows over an Airfoil

R. Magnus* and H. Yoshihara†
General Dynamics Convair Division, San Diego, Calif.

Inviscid, transonic flows over the NACA 64A410 airfoil were calculated using a finite-difference analog of the Euler equations. Steady flow solutions were obtained for angles of attack of 0°, 2° and 4° at Mach 0.72. Unsteady calculations were made at the same Mach number and in the same general angle-of-attack range for a step change of angle of attack, a step change in pitching angular velocity, and for sinusoidal pitching oscillations about the midchord at reduced frequencies 0.2, 1.0, and 5.0. (Reduced frequency, $K \equiv \omega C/U_\infty$.) A summary of the resulting surface pressures, shock locations, and the forces and moments is presented. The forces and moments obtained for the cases with harmonic oscillations were compared to the results from a linearized analysis which used, to approximate the indicial functions, the responses calculated for the step changes.

Introduction

NUMERICAL solutions of transonic flows about harmonically oscillating airfoils have been obtained by Ehlers[1] and Traci, et al.[2] In these two works, the solutions were obtained by solving in turn, first, the steady, nonlinear, transonic perturbation potential equation to obtain a steady, background flow; and second, a linear, potential equation for the unsteady, small perturbation about the background flow. The boundary conditions for both equations were satisfied along the airfoil chordline slit.

In the work to be described here, unsteady, transonic flows over an airfoil are calculated using a finite-difference analog of the Euler equations, and the airfoil boundary conditions are satisfied along a fixed, curved contour that matches the airfoil shape. The procedure used is an extension of the method described in our earlier report on steady, transonic flow over airfoils.[3]

In that it uses the Euler equations and does not rely on linearization, the present method can be applied to problems for which the small-disturbance methods would not be suitable. For example, problems involving angle-of-attack changes that cause the shocks to move appreciably can be calculated. Alternatively, problems on harmonically oscillating airfoils can be solved and the results examined to determine nonharmonic features of the response - features that would be absent in the linearized solutions. By satisfying boundary conditions on an airfoil-shaped contour, the present method avoids the uncertainties that occur in the perturbation methods because of approximate, numerical handling of the singularity at the forward end of the chordline slit.

In undertaking the present work, it was recognized that the calculations would probably be too expensive for routine use. Our intention was to generate a few solutions that would show typical features of the flows and might serve as comparison solutions for simpler, more approximate methods.

The calculations were done on the CDC 7600 computer at the University of California, Lawrence Berkeley Laboratory, using remote terminal facilities. The longest problem, sinusoidal oscillation at reduced frequency 0.2, required seven hours of computing. We have subsequently determined that this problem can be done in two hours if the program is compiled using optimization procedures specifically attuned to the characteristics of the CDC 7600.

Presented as Paper 75-98 at the AIAA 13th Aerospace Sciences Meeting, Pasadena, California, January 20-22, 1975; submitted February 10, 1975; revision received July 21, 1975. This work was done for the Office of Naval Research (Fluid Dynamics Program), Department of the Navy, under Contract N00014-73-C-0294. We also are indebted to the staff of the Computational Fluid and Dynamics Branch of the NASA Ames Research Center for their advice and assistance.

Index categories: Nonsteady Aerodynamics; Subsonic and Transonic Flow; Computer Technology and Computer Simulation Techniques.

*Senior Staff Scientist, Aerodynamics.

†Engineering Staff Specialist, Engineering Technology. Associate Fellow AIAA.

Notes on the Method of Solution

Equations

The unsteady Euler equations were used in the form of the conservation laws

$$\partial(\rho)/\partial t = -\partial(\rho u)/\partial x - \partial(\rho v)/\partial y \quad (1)$$

$$\partial(\rho u)/\partial t = -\partial(\rho u^2 + p)/\partial x - \partial(\rho uv)/\partial y \quad (2)$$

$$\partial(\rho v)/\partial t = -\partial(\rho uv)/\partial x - \partial(\rho v^2 + p)/\partial y \quad (3)$$

$$\partial(E)/\partial t = -\partial[u(E+p)]/\partial x - \partial[v(E+p)]/\partial y \quad (4)$$

Here, ρ, p, u, v, x and y have the meanings standard in fluid-mechanics problems, and E is the total energy per unit volume

$$E \equiv p/(\gamma - 1) + (\rho/2)(u^2 + v^2) \quad (5)$$

For the steady-flow calculations, the uniform total-enthalpy condition

$$(u^2 + v^2)/2 + \gamma p/[(\gamma - 1)\rho] = H_T \quad (6)$$

was used with differential Eqs. (1), (2), and (3).

Difference Scheme

An explicit two-step, finite-defference scheme of the Lax-Wrendroff type was used. The scheme is the one described by Thommen[4] and has been adapted for the present work by dropping the true viscous terms and substituting a diffusion in the same fashion as in our earlier work.[3] The diffusive damping was used in the region of the shock.

Grid Arrangement

The geometric field is covered with a number of grids having a total of about 6000 nodes. Most of the points are in square Cartesian mesh systems, but sheared meshes of the general type described by Jameson[5] are also used along the airfoil surface. The bulk of the iterative calculations are done in the simple Cartesian grids. The general mesh arrangement principles are illustrated by Fig. 1.

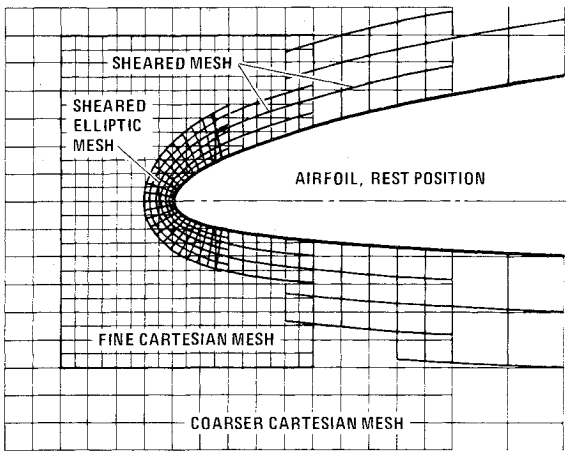

Fig. 1 Grid arrangement principles.

The coarsest mesh, used in the outer part of the field, has a spacing of 0.4 chord. Finer mesh systems are imbedded in the coarser ones to provide the desired detail in the vicinity of the airfoil. Around the airfoil as a whole the basic mesh has 0.05 chord spacing, and finer mesh as small as 0.00625 chord spacing is used near the nose. Similarly, mesh with $\Delta x = 0.0125$ chord is used above the aft part of the airfoil to provide the desired resolution of the shock. Around the nose, a sheared elliptic system is used so that near the minimum radius of curvature of the airfoil, the mesh has a minimum spacing of 0.0017 chord.

The spacing in each coarser Cartesian mesh is a power of two larger than the spacing in each finer mesh, and lines of the coarser meshes form the perimeter lines and some of the interior lines of the finer meshes. This conformation of grids makes the data exchanges between the various systems simple and also simplifies the synchronization of the calculations that progress at different rates in the various grids.

Waves propagating in one grid may be partially reflected when passing into another grid of different coarseness because of inevitable differences in the dispersive and diffusive truncation errors for the two systems.

Synchronization

With an explicit differencing scheme, the calculation is stable only if the time step is limited. Based upon typical expected flow conditions and a knowledge of the characteristics of the scheme, Δt was set at 0.25 Δx; here, a time unit is defined as C/a^*_∞ where C is the airfoil chord and a^*_∞ is the critical speed in the free stream.

In advancing the solution in a finer mesh region imbedded in a (say, twice greater mesh-size) coarser region, two time steps are made in the finer region for each one in the coarser. Thereafter, the two solutions are adjusted by an exchange of data. The solution in the finer mesh is assigned to replace the coarser mesh solution at corresponding points in the interior of the finer mesh, and the solution in the coarser mesh is interpolated onto the perimeter of the finer mesh region. Similar principles are used in exchanging data between the Cartesian and the sheared regions.

Boundary Conditions

The problems treated here all deal with rigid body motion of the profile. The mesh system is left unaltered in time, and the airfoil boundary condition is satisfied at those mesh nodes that lie on the surface of the airfoil in its rest attitude. Transferring of position in the field at which boundary conditions will be satisfied is a procedure much used in fluid mechanics; the basis for it is discussed by VanDyke.[6]

The values of the dependent variables at the airfoil nodes are found by a sequential process: a) A one-sided, finite-difference procedure (obtaining data only from the exterior of the airfoil) is used to obtain tentative values for the density, energy, and velocity components. b) The flow velocity component along the instantaneous surface normal is adjusted to match the airfoil mechanical velocity in that direction. The adjustment alters the normal velocity, density, and energy in the manner that they would be altered by a plane isentropic wave propagating outward from the surface.

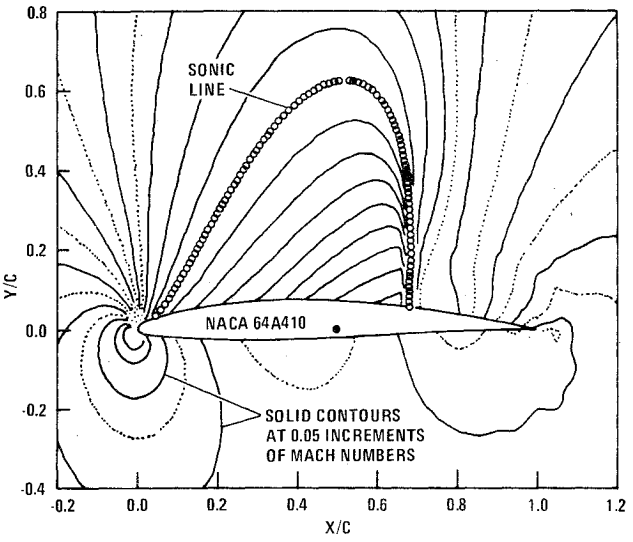

Fig. 2 Isobars of the steady flow at Mach 0.72 and $\alpha = 2°$

This manner of satisfying boundary conditions has been used in our earlier work[3] and has been studied by Abbett.[7] An isentropic wave is adequate because the maximum strength expected for the adjustment waves (occurring when the angle of attack is suddenly changed by 2°) corresponds to a shock Mach number of about 1.015.

At the perimeter of the computation field, which is 9.6 chords square, flow properties have been held to assigned values throughout the process of solving a given unsteady problem. The distributions for flow properties were obtained by adding perturbations due to a vortex and doublet (at the airfoil) to the free-stream conditions. The vortex strength was fixed at the value corresponding to the airfoil lift at a 2° angle of attack.

The distances to the field boundaries and disturbance propagation speeds are such that the results at the airfoil should be free of disturbances reflected from the boundary for about thirteen time units after the initial perturbation. The solutions for the problems on sinusoidally-oscillating airfoils have been followed for more than thirteen time units and, therefore, contain the influences of the perimeter boundary condition.

Calculations Carried Out

The steady flow over the airfoil was calculated for angles of attack of 0, 2, and 4°. The airfoil shape and the general nature of the steady flow over the airfoil at a 2° angle of attack are shown in Fig. 2. Here, the isobars indicated by solid lines are for those pressures (in an isentropic flow) corresponding to Mach numbers at 0.05 intervals. The pressure distributions at the three angles of attack are shown in Fig. 3. The shock locations and the aerodynamic coefficients obtained by integrating pressures are given in Table 1.

Calculations were made of the unsteady flow over the airfoil oscillating sinusoidally in pitch about the midchord point. The mean angle of attack was 2° and reduced frequencies (K) of 0.2, 1.0, and 5.0 were calculated with amplitudes (Amp) of 2.0, 2.0, and 0.4° respectively, where

$$K \equiv \omega C / U_\infty \tag{7}$$

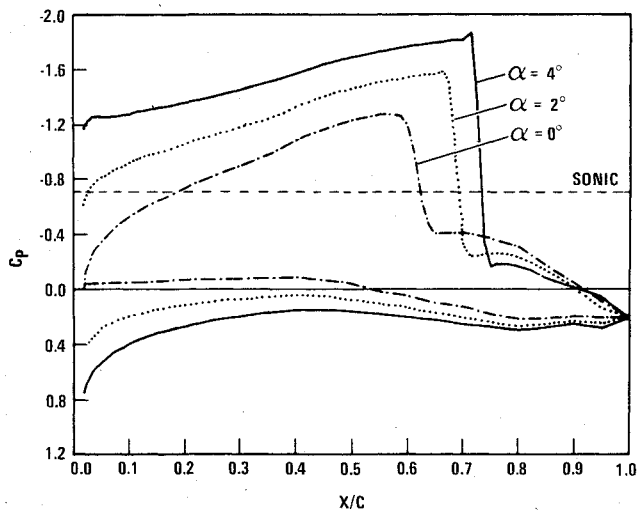

Fig. 3 Pressure distributions in steady flow.

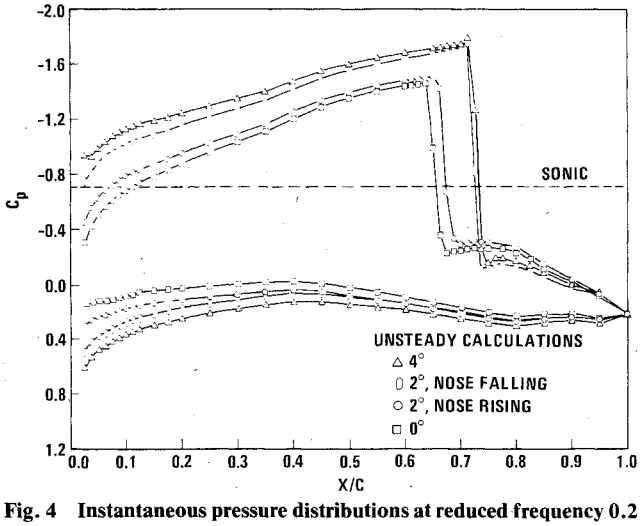

Fig. 4 Instantaneous pressure distributions at reduced frequency 0.2

$$\alpha(t) = 2.0 + \text{Amp} \cdot \sin(\omega t) \tag{8}$$

The oscillatory calculations were started from the steady flow solutions for $\alpha = 2°$ and were continued until a repeatable response was obtained. The pressures at four places in the cycle for the $K = 0.2$ case are shown in Fig. 4 to illustrate typical results.

The responses to step changes in angle of attack and in pitching angular velocity were calculated, and the results for normal force and pitching moment are given in Figs. 5 and 6. The magnitude of angular-velocity jump is the maximum encountered in the sinusoidal oscillatory cases treated. Since the circulation used in calculating the field perimeter boundary condition was left at the value corresponding to C_N for a 2° angle of attack, the response traces should approach final values somewhat lower than the values that would be achieved in a proper calculation of the steady state.

Table 1 Calculated properties in steady flow, NACA 64A410, March 0.72

Angle of Attack	C_N	C_x	$C_m(C/4)$	Shock X/C
$\alpha = 4°$	1.3928	-0.0277	-0.2186	0.7330
$\alpha = 2°$	1.0385	-0.0104	-0.1770	0.6920
$\alpha = 0°$	0.6544	0.0053	-0.1440	0.6228

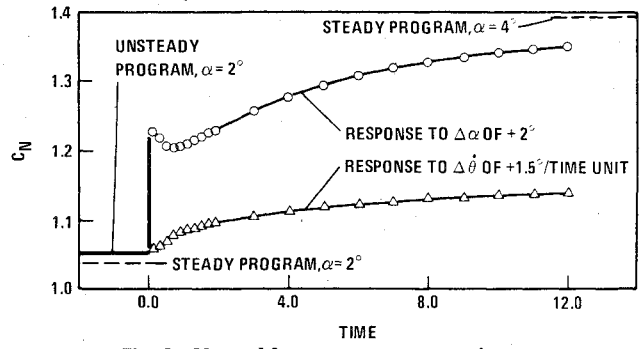

Fig. 5 Normal force responses to step inputs.

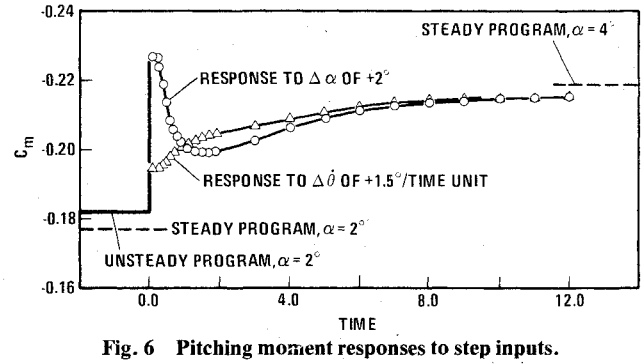

Fig. 6 Pitching moment responses to step inputs.

In Figs. 5 and 6, the airfoil, at Mach 0.72, would move one chord length through the atmosphere in 1.33 time units. Because the steady and unsteady programs use different forms of the energy equation, the trunction errors of the two systems are not identical, and small differences between the results of calculating the steady flow with the two programs will occur.

Observations on the Results

Steady Flow

In Table 1 it can be seen, by inspecting the increments between values at the successive angles of attack, that the pitching moment and the location of the shock are noticeably nonlinear functions of the angle of attack over the range considered.

Unsteady Forces, Moments, and Shock Locations

For the cases with sinusoidal pitching oscillations, the force and moment coefficients and the shock locations as functions of time were assumed representable by truncated Fourier series

$$f(t) = B_0 + \sum_{n=1}^{4} A_n \sin(n\omega t + \phi_n) \tag{9}$$

Approximating traces of this type were fitted to the calculated responses by a least-squares procedure, and the fitted parameters are listed in Table 2.

Inspection of the relative amplitudes of the four harmonics of each fitted trace shows that, for the normal force and pitching moment, the amplitudes of the higher harmonics are all less than 0.05 of the amplitudes of the respective fundamentals. The shock location traces all have second harmonics whose amplitude is greater than 0.05 of the fundamental amplitude, and two of the responses in axial force coefficient also do.

The movement of the shock is of significance in determining the pitching moment at $K = 0.2$ but is unimportant at

Table 2 Responses to sinusoidal oscillations represented by four harmonics

Reduced Frequency (K)	Mean Value (Bo)	Amplitudes A_1	A_2	A_3	A_4	Phase Angles (Deg) ϕ_1	ϕ_2	ϕ_3	ϕ_4
	Normal Force Coefficient, C_N								
0.2	1.05206	0.25870	0.00639	0.00183	0.00091	-22.81	23.31	-131.06	122.53
1.0	1.05843	0.14729	0.00046	0.00013	0.00004	-2.09	25.41	106.86	76.46
5.0	1.05570	0.04382	0.00016	0.00021	0.00002	7.62	-5.30	-169.49	-24.25
	Axial Force Coefficient, C_x								
0.2	-0.00834	0.00910	0.00119	0.00020	0.00010	150.41	98.78	-134.58	108.06
1.0	-0.00889	0.00914	0.00055	0.00004	0.00001	129.88	0.82	-0.17	-2.74
5.0	-0.01083	0.00311	0.00002	0.00001	0.00000	78.43	-86.06	-173.78	
	Negative Pitching Moment Coefficient, C_m (C/4)								
0.2	0.18356	0.03109	0.00152	0.00095	0.00034	-17.04	128.25	-123.97	120.93
1.0	0.18297	0.02778	0.00045	0.00002	0.00001	59.43	176.17	97.25	16.52
5.0	0.18039	0.01748	0.00006	0.00007	0.00001	47.80	14.70	-168.32	-2.88
	Locations of Upper Surface Shock, X/C								
0.2	0.69609	0.04460	0.00700	0.00119	0.00081	-33.25	36.05	-162.91	113.85
1.0	0.70118	0.01055	0.00096	0.00033	0.00016	-82.63	-97.77	127.53	-77.54
5.0	0.69817	0.00092	0.00008	0.00012	0.00001	-34.18	10.26	-159.15	74.80

$K=5.0$. For steady flow at $\alpha=2°$, the difference between C_p ahead of and behind the shock is about 1.3 and the shock is located at about 0.69 chord (see Fig. 3). Using the data on shock movement from Table 2, the pitching moment excursions (moments about the quarter chord) due to the shock movement have amplitudes that are, roughly, 0.8, 0.2, and 0.03 of the amplitudes of the overall pitching moment excursions at $K=0.2$, 1.0, and 5.0, respectively. The speed of the shock in its fore-and-aft translational motion, as viewed in airfoil-fixed coordinates, did not exceed 0.01 of the free-stream sound velocity.

Unsteady Surface Pressures

Fourier coefficients, as described above, were also fitted to the pressure histories at 40 locations on the airfoil surface. In general, the amplitudes of the higher harmonics of the pressure excursions are less than 0.05 the amplitudes of the fundamentals. This is not true, of course, at locations traversed by the moving shock. It also was found that, on the upper airfoil surface aft of the shock, the amplitudes of the second harmonics of the pressure excursions were about 0.2 of the amplitudes of the fundamentals. Figures 7-11 give a general view of the amplitudes and phases of the presssure excursions at various locations on the airfoil. Figures 7-9 show the locations in the cycle at which the maximum and minimum pressures occurred (as determined by inspection of the calculated response traces).

At the lowest reduced frequency, $K=0.2$, the pressure extremes occur within 40° of the angle-of-attack extremes except in the region aft of the shock on the upper surface. This behavior of the pressures aft of the shock is in concordance with the arrangement of the pressure traces expected in quasisteady flow (see Fig. 3).

At the higher reduced frequencies the "piston" pressures become important near the ends of the airfoil, and the presssure extremes there tend to occur near the 0 and 180° points of the cycle, i.e., where the plunging velocities are at their highest. The chordwise distributions of the double am-

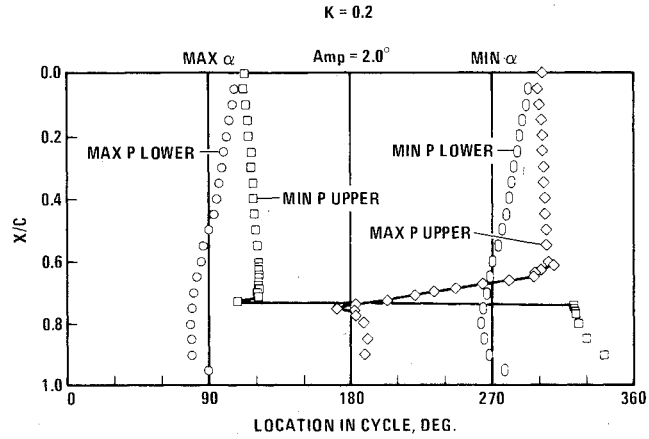

Fig. 7 Locations in the cycle at which pressure extremes occur, $K=0.2$.

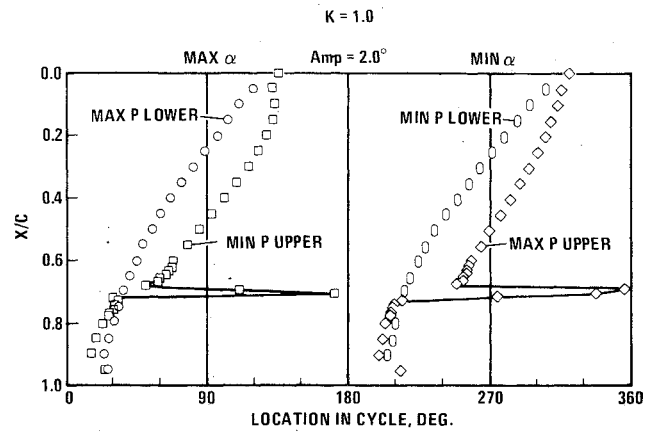

Fig. 8 Locations in the cycle at which pressure extremes occur, $K=1.0$.

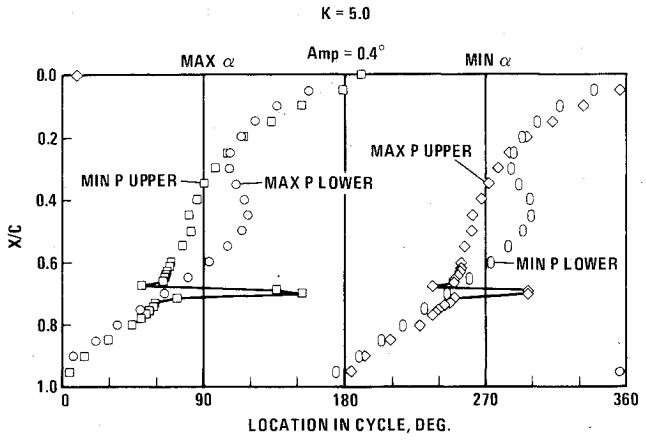

Fig. 9 Locations in the cycle at which pressure extremes occur, $K = 5.0$.

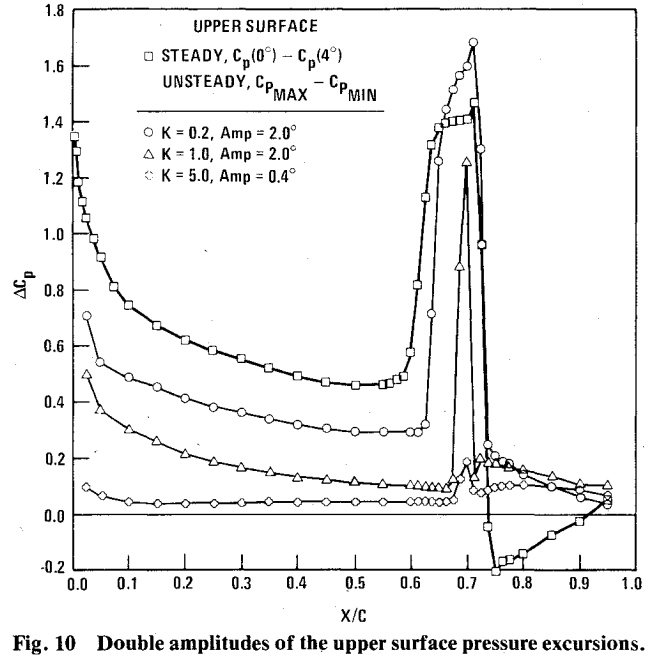

Fig. 10 Double amplitudes of the upper surface pressure excursions.

plitudes of the pressure excursions are shown in Figs. 10-11. The large peaks near 0.7 chord on the upper surface are caused by shock movement.

Nonlinear Response

The response of a linear system being driven sinusoidally should be sinusoidal with, possibly, a phase shift. The presence of higher harmonics in the response traces is evidence of nonlinearity in the system. Inasmuch as the pitching moment and the shock location are nonlinear functions of the angle of attack in steady flow, it is not surprising, when the airfoil is oscillated sinusoidally in pitch, to see appreciable higher harmonics in some of the response traces. Some traces having different degrees of nonsinusoidal response at reduced frequency 0.2 are shown in Figs. 12-13; the light solid lines are single harmonics fitted to the response traces by a least-squares procedure. At reduced frequencies 1.0 and 5.0, however, the higher harmonics tended to be unimportant except for those in the shock movement; see Table 2.

Figure 12 illustrates that, while the pressure upstream of the shock ($X/C = 0.6$) varies quite sinusoidally, the pressure downstream ($X/C = 0.75$) does not. This feature occurs because the pressure at the downstream side of the shock is a nonlinear function of the Mach number just ahead of the shock.

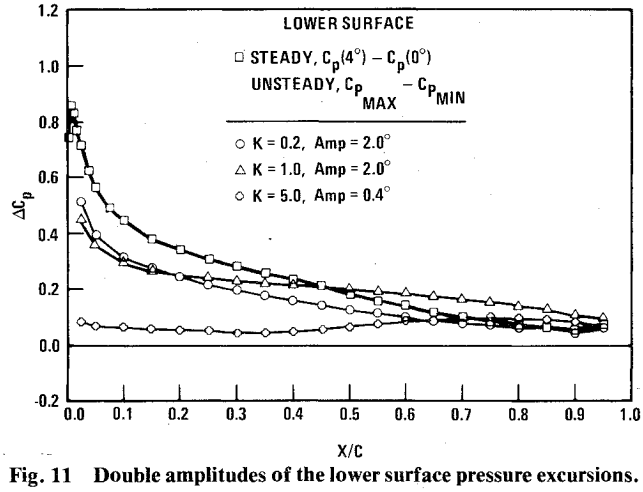

Fig. 11 Double amplitudes of the lower surface pressure excursions.

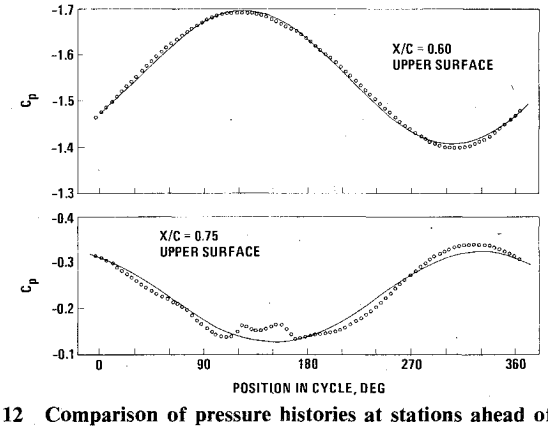

Fig. 12 Comparison of pressure histories at stations ahead of and behind the shock, $K = 0.2$

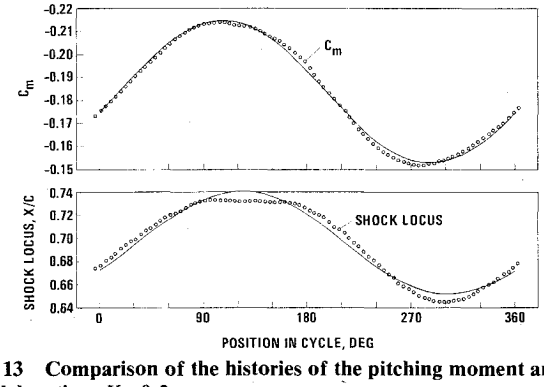

Fig. 13 Comparison of the histories of the pitching moment and the shock location, $K = 0.2$.

Figure 13 shows the shock locus on the upper surface and the pitching moment coefficient. Since having the shock move aft causes a negative pitching moment, the rough correlation in phase of shock movement with the pitching moment at reduced frequency 0.2 should be apparent. Note that the shock remains close to its most aft location for almost a quarter of the oscillation cycle. The nonsinusoidal shock movement is probably also a consequence of the nonlinearity of the presssure recovery as a function of the shock Mach number.

Linear System Studies

That the response of the normal force and pitching moment, when the airfoil is subjected to an arbitrary forcing function, might be calculable from the responses to step

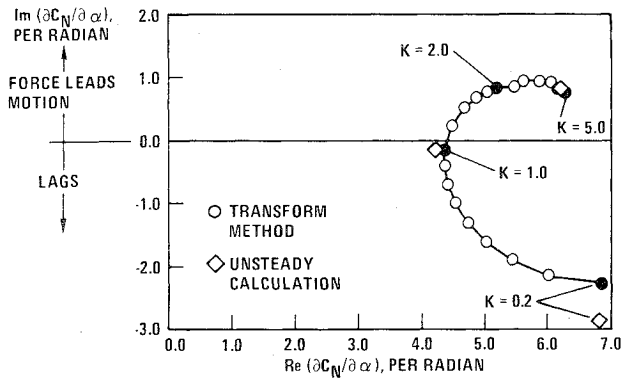

Fig. 14 Response of the normal force to sinusoidal pitching oscillations about mid-chord.

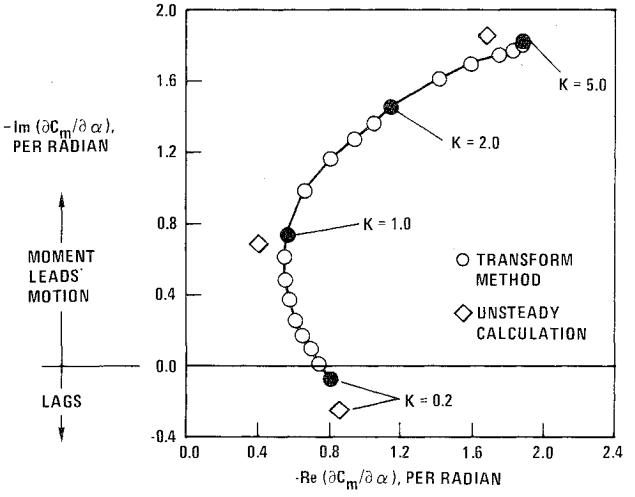

Fig. 15 Response of the pitching moment to sinusoidal pitching oscillations about mid-chord.

changes by use of convolution integrals, as is possible in truly linear systems, was investigated. It is recognized that the system being dealt with is not strictly linear, that the indicial responses available are for rather large step changes, and that the step changes have been made only in one direction so that directional bias may be a factor.

The indicial responses were calculated out to 12.0 time units and should be free of undesired influence from the perimeter boundary condition. Curves of the form

$$f(t) = \Delta f\,(1.0 - \exp(-K_1 t - K_2)) \qquad (10)$$

were fitted to the last parts of the response traces and used for extrapolating the response functions. Here, the magnitude Δf establishing the final value of f was presumed known, and the parameters K_1 and K_2 were chosen to make the curve fit the latter portion of the calculated response trace.

Using the indicial response traces described above, the responses to steady sinusoidal forcing functions at reduced frequencies from 0.2 to 5.0 were calculated. The Laplace transform methods described by Gardner and Barnes[8] were used. The responses per radian amplitude of the pitching oscillations (about the midchord point) are shown in Figs. 14-15 in complex form. The real part represents the portion in phase with the motion and the imaginary part represents the component leading the motion by 90°. In these two figures, the values of the unlabelled reduced frequencies may be deduced by assuming uniform increments between the tagged frequencies.

The responses to sinusoidal forcing calculated with the full unsteady program have some higher harmonics; arbitrarily, the responses have been characterized by the parameters of pure sinusoids fitted by a method of least squares. This data is compared with the responses generated from the indicial responses by the linear-transform method. In the case of the normal force (Fig. 14), the maximum disagreement between the two methods is a vector whose magnitude is no more than 0.08 of the basic response vector. For the pitching moments (Fig. 15), The magnitude of the disagreement between the two methods is 0.22 of the magnitude of the basic response.

Similarly, constructing the responses of surface pressures, for steady, sinusoidal oscillations of the airfoil, from the indicial response traces gave values in relatively good agreement with the full, unsteady calculations except along the upper surface aft of the shock at reduced frequency 0.2.

Concluding Remarks

Approximations

Here, as in other numerical solutions of complex problems, choices had to be made on the increments used in the discretization, on the procedures to stabilize the calculations, and on the approximations used in satisfying the boundary conditions.

We elected to satisfy airfoil boundary conditions in quasiplanar fashion on a fixed, curved contour having the airfoil shape rather than on the moving airfoil surface. Higher order terms of a Taylor expansion could be introduced into the boundary condition to account for the transfer in locations at which the boundary conditions are satisfied, but we have not tried this procedure. The effects of imposition of the steady boundary condition on the perimeter of the field also have not been checked by repeating the calculations with the perimeter moved farther from the airfoil.

Conclusions

Based upon the calculations of inviscid flows that have been carried out, a number of conclusions may be drawn that might be of interest in deciding on a simpler, analytic method: For the lowest frequency pitching oscillations, $K = 0.2$, the movement of the shock is an imporatant factor in determining the pitching moment excursions. Shock movement was unimportant at $K = 5.0$.

Unsurprisingly, when the airfoil was pitched sinusoidally and the various response traces were examined, higher harmonic components that would indicate nonlinear behavior tended to be most prevalent in the traces for those quantities such as shock location, which were known to be nonlinear functions of angle of attack in steady flow. The pressure recovery that can be achieved behind a normal shock is a nonlinear function of the pressure just ahead of the shock; this is the cause for the pressure oscillations aft of the shock being nonsinusoidal when the airfoil is pitched sinusoidally. Unless shock-jump conditions were imposed, this nonlinearity would not appear prominently in a calculation based on the potential flow equation.

When the normal force responses to sinusoidal pitching were constructed by using the indicial responses and convolution integrals appropriate for linear systems, the results agreed within about 0.08 of the basic normal force response. For the pitching moment, the disagreement between the two methods was as much as 0.22 of the basic value. The possibility that the indicial response traces might be useful in constructing responses to arbitrary forcing functions of small amplitude has not been investigated.

Cautions

These inviscid calculations are not presented as a representation of what might be seen in tests of this airfoil in a wind tunnel or in flight. The airfoil is of a family that is in use on present-day aircraft, and the Mach number and angles of at-

tack considered in the calculations might reasonably occur in flight. The loading on the upper surface as determined by the inviscid calculations, however, is not what should be expected under experimental conditions. The interaction of the shock with the boundary layer is strong enough to alter the airfoil pressure distribution substantially. It is typical to find, in experiments on this airfoil, that the shock is not further aft than about 0.6 chord and that the Mach number ahead of the shock is not greater than about 1.33 for the Mach number and in the angle-of-attack range we have considered. We feel that most of the currently available methods for calculating steady and unsteady supercritical flows over airfoils do not incorporate the effects of the shock interacting with the boundary layer in a realistic fashion. Definitely, further research on the interaction in needed.

References

[1]Ehlers, F.E., "A Finite Difference Method for the Solution of Transonic Flow Around Harmonically Oscillating Wings," NASA, CR 2257, July 1974.

[2]Traci, R.M., Albano, E.D., Farr, J.L., Jr., and Cheng, H.K., "Small Disturbance Transonic Flows About Oscillating Airfoils," AFFDL-TR-74-37, June 1974, Air Force Flight Dynamics Laboratory, Wright-Patterson Air Force Base, Ohio.

[3]Magnus, R. and Yoshihara, H., "Inviscid Transonic Flow Over Airfoils," *AIAA Journal*, Vol. 8, Dec. 1970, pp. 2157-2162.

[4]Thommen, H.U., "Numerical Integration of the Navier-Stokes Equations," *Zeitschrift fur angewandte Mathematik und Physik*, Vol. 17, May 1966, pp. 369-384.

[5]Jameson, A., "Iterative Solution of Transonic Flows over Airfoils and Wings, Including Flows at Mach 1," *Communications in Pure and Applied Mathematics*, Vol. XXVII, May 1974, pp. 283-309.

[6]VanDyke, M., *Perturbation Methods in Fluid Mechanics*, Academic Press, New York, 1964.

[7]Abbett, M.J., "Boundary Condition Computational Procedures for Inviscid, Supersonic Steady Flow Field Calculations," NASA. CR-114446, Nov. 1971.

[8]Gardner, M.F. and Barnes, J.L., *Transients in Linear Systems, Volume I, Lumped-Constant Systems,* Wiley, N. Y., 1942.